Neutrophil β1 adrenergic receptor blockade blunts stroke-associated neuroinflammation

SUPPLEMENTAL MATERIAL

SUPPLEMENTAL FIGURES

Graphical abstract. β1AR blockade by metoprolol ameliorates brain I/R injury.

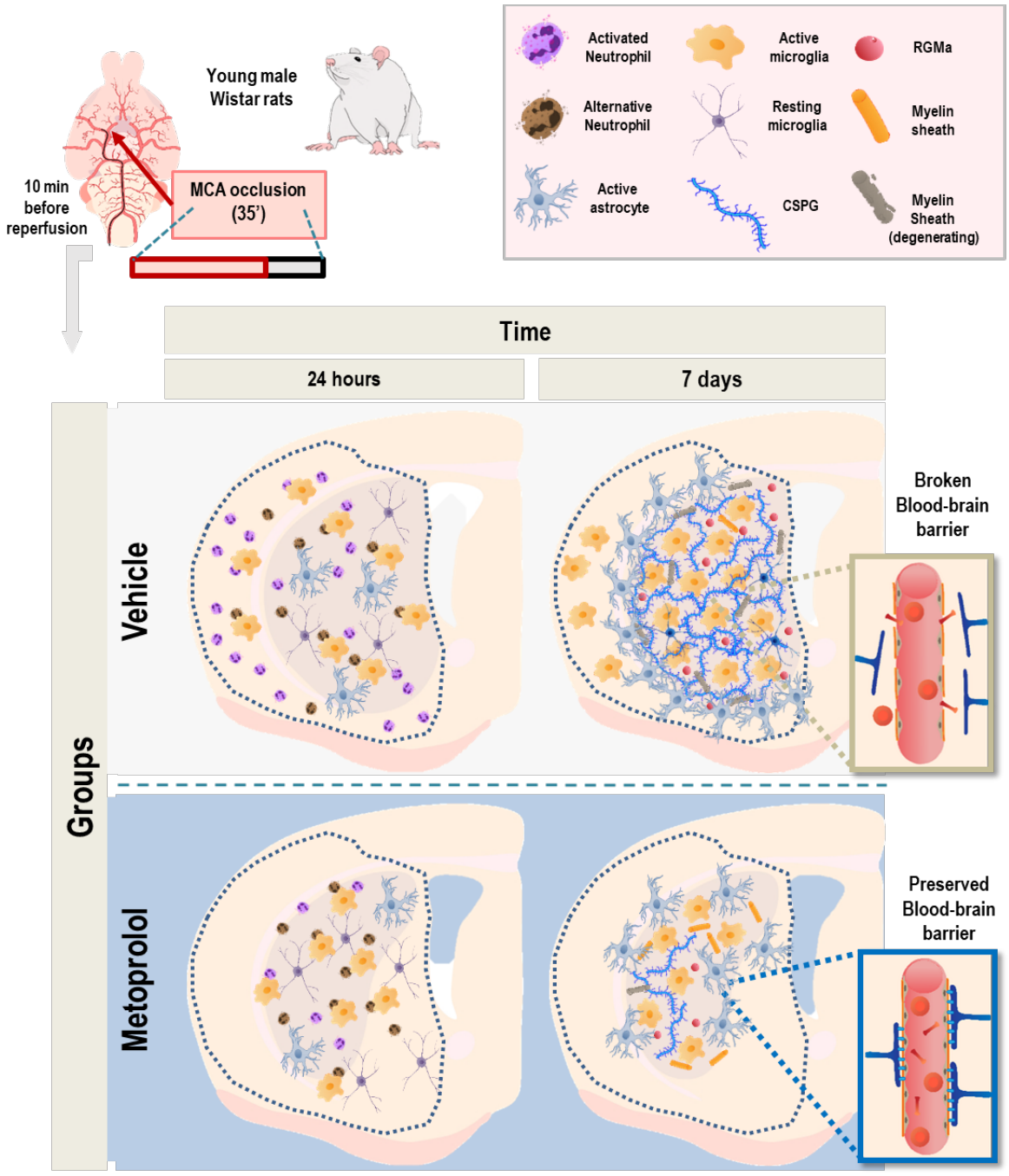

By attenuating acute neutrophil infiltration via β1AR, metoprolol reduces brain infarct size, prevents neuronal loss and cerebral edema progression. As a consequence of neutrophil stunning, metoprolol counteracts the pro-inflammatory state while conserving a subset of alternative neutrophils in brain,

which contribute to create a pro-resolving microenvironment that favors long-term recovery. This results in better preservation of blood-brain barrier integrity and reduced subacute neuroinflammation (microglia/macrophage pro-inflammatory responses, proteoglycan deposition, glial scarring and myelin sheath degeneration). Therefore, metoprolol is a promising candidate for testing in clinical trials of patients with suspected ischemic stroke.

Supplemental Fig. 1

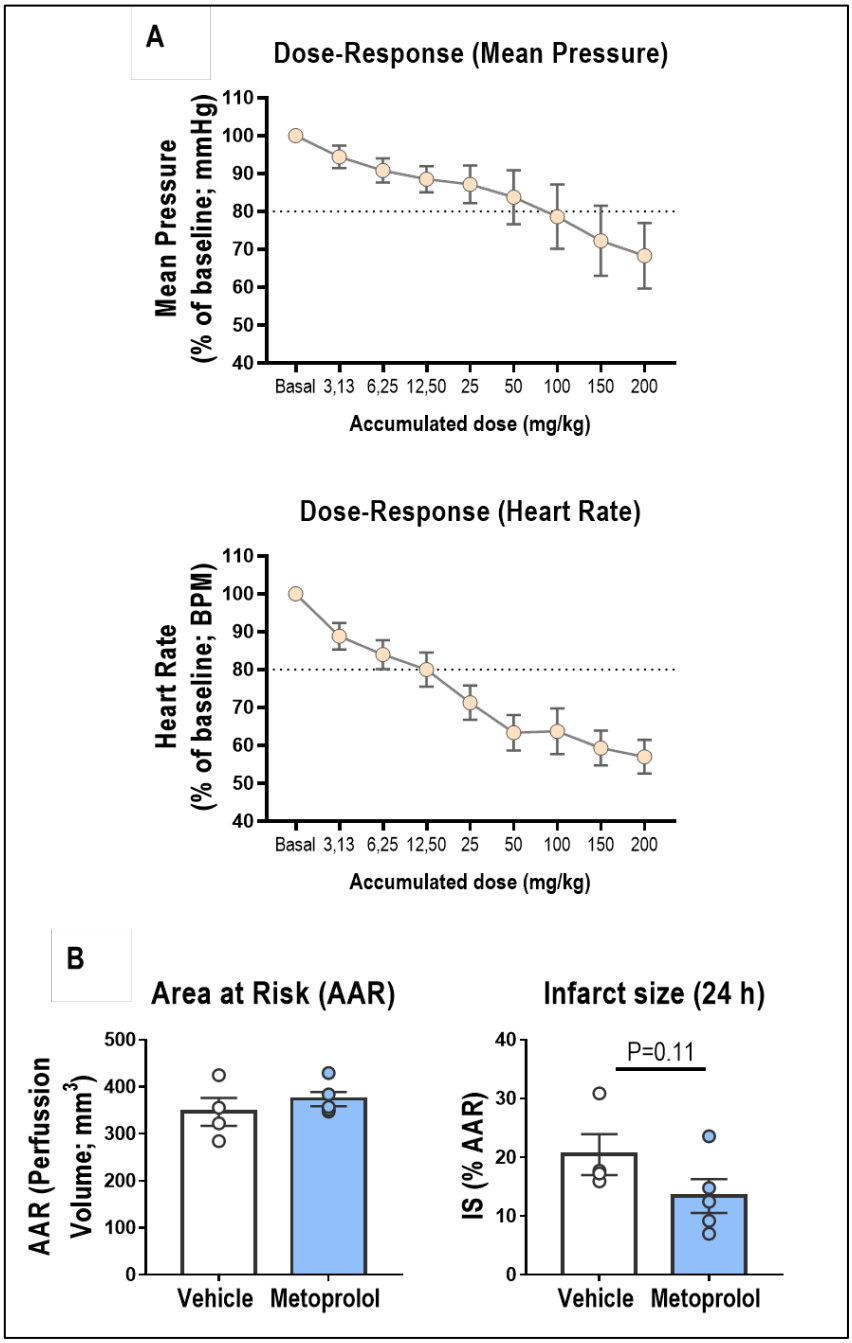

(**A**) The hemodynamic study of 8 different doses of metoprolol (3.13, 6.25, 12.5, the formerly chosen dose, 25, 50, 100, 150 and 200 mg/Kg). Intravenous 12.5 mg/kg dose of metoprolol induced a moderate hemodynamic effect, as indicated by decrease in heart rate (bpm) and arterial pressure (mmHg) of less than 20%. These data support the selection of 12.5 mg/Kg i.v. injection for the experimental model of ischemic stroke. n=5 animals. (**B**) Infarct size (IS) evaluated by coronal T2W

MRI at 24 h (vehicle, n=5; metoprolol, n=5; 1 rat excluded upon confirmation of the absence of artery occlusion). Final IS was calculated as the ratio of infarct volume to the area-at-risk (AAR) and expressed as %. A lower dose of metoprolol (6.25 mg/Kg) tended to decrease IS, although no significant differences were observed. Data are presented as mean±SEM.

Supplemental Fig. 2.

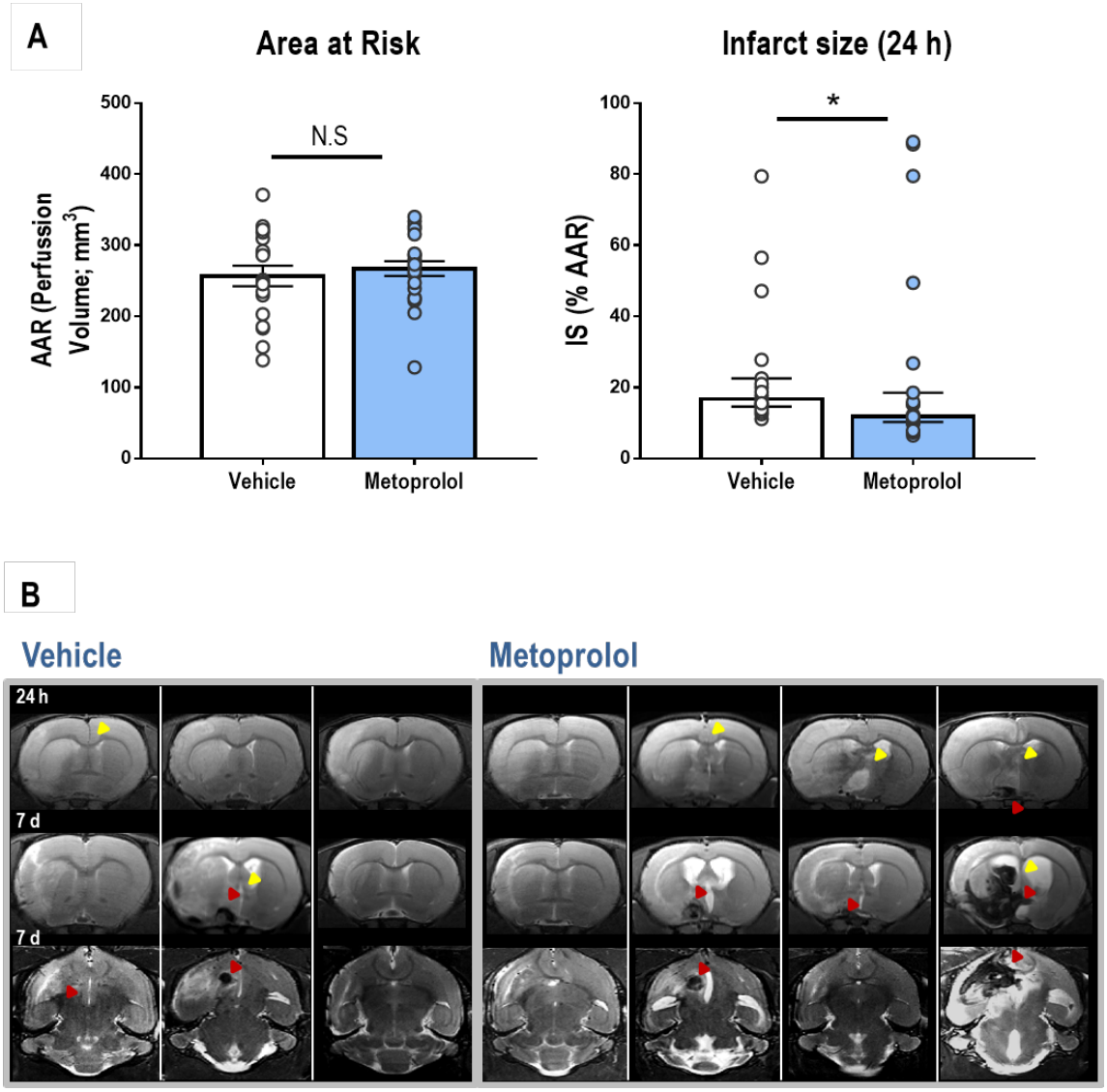

(**A**) Area at risk (AAR), determined by dynamic susceptibility contrast perfusion imaging, and infarct size assessed by coronal T2-weighted (T2W) MRI at 24 h post-reperfusion (vehicle, n=19; metoprolol, n=23). Infarct size was calculated as the ratio of infarct volume to the AAR and expressed as a percentage. After inclusion of all rats in the statistical analysis (including those with IS > 40%), the significant difference ($p<0.05$) was maintained between rats receiving pre-reperfusion vehicle or metoprolol. Dots correspond to individual rats, column heights to median values, and whiskers to interquartile range. *$p<0.05$; unpaired Mann-Whitney test. (**B**) T2W MRI at 24 h post-reperfusion (top row; coronal plane) and 7 d post-reperfusion (middle and bottom rows; coronal and axial planes, respectively) in vehicle-treated rats (left) and metoprolol-treated rats (right) with IS >40%. Infarct

regions correspond to hyperintense areas. Rats with IS >40% also showed a midline shift (yellow arrowheads) or hemorrhage (red arrowheads) at 7 d post-reperfusion.

Supplemental Fig. 3.

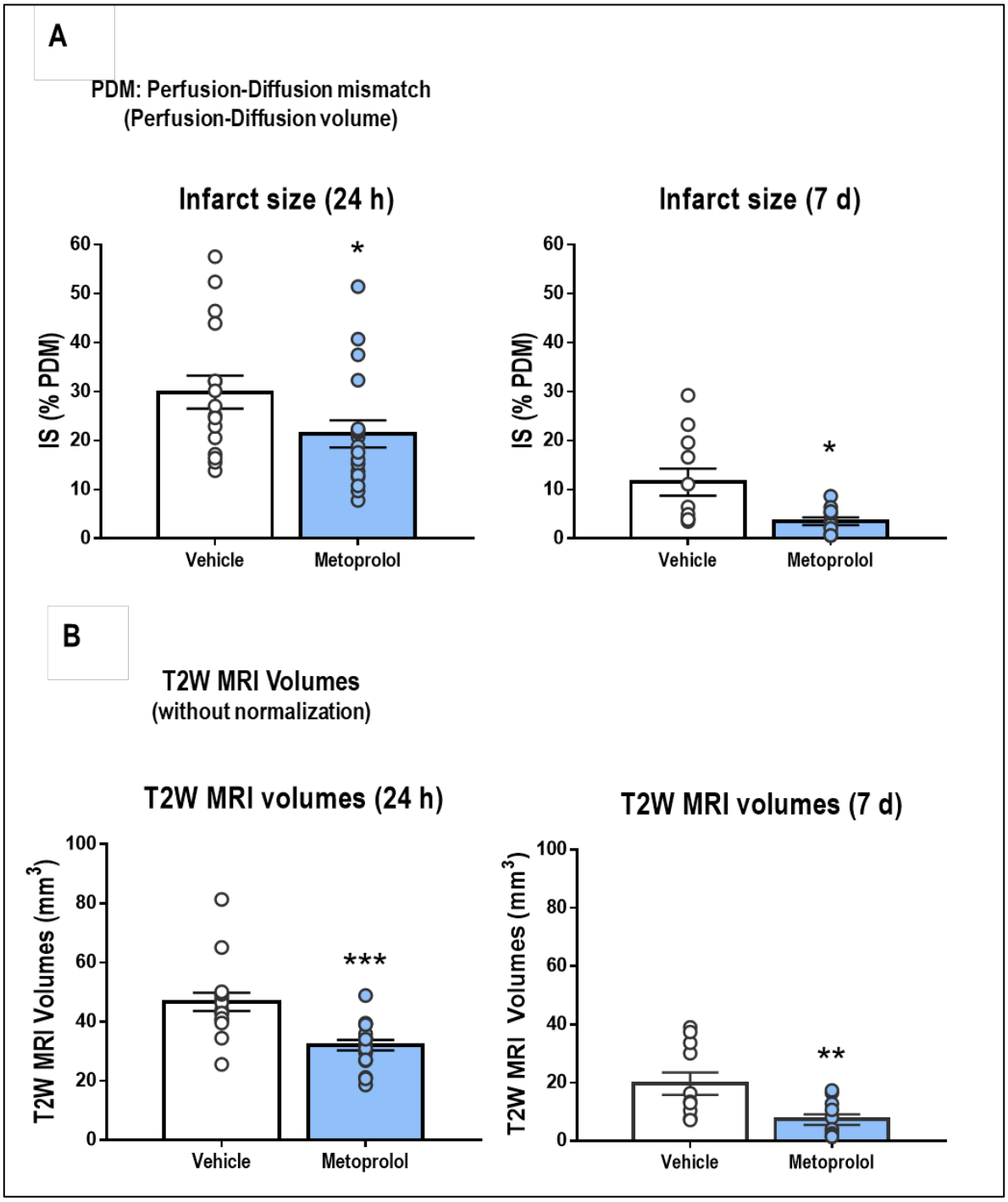

(**A**) Infarct size (IS) normalized to at-risk-to-infarction tissue assessed as perfusion-diffusion mismatch (PDM). The results were similar to those obtained by normalization to area-at-risk (AAR) (see Fig. 1) at 24 h post-reperfusion (vehicle, 29.9 ± 3.39%; metoprolol, 21.4 ± 2.79%; $p<0.05$) and 7 d post-reperfusion (vehicle, 11.5 ± 2.78%; metoprolol, 3.55 ± 0.78%; $p<0.05$) (**b**) Non-normalized T2-

weighted MRI infarct volumes; the benefit of metoprolol is still evident at 24 h post-reperfusion (vehicle, 46.7 ± 3.11 mm^3; metoprolol, 32.0 ± 1.77 mm^3; $p<0.005$) and 7 d post-reperfusion (vehicle, 19.6 ± 3.84 mm^3; metoprolol, 7.29 ± 1.83 mm^3; $p<0.05$), indicating that IS was not conditioned by either AAR or PDM. Data are means ± S.E.M. *p<0.05, **p<0.01, ***p<0.005; unpaired Mann-Whitney or Student *t*-test.

Supplemental Fig. 4.

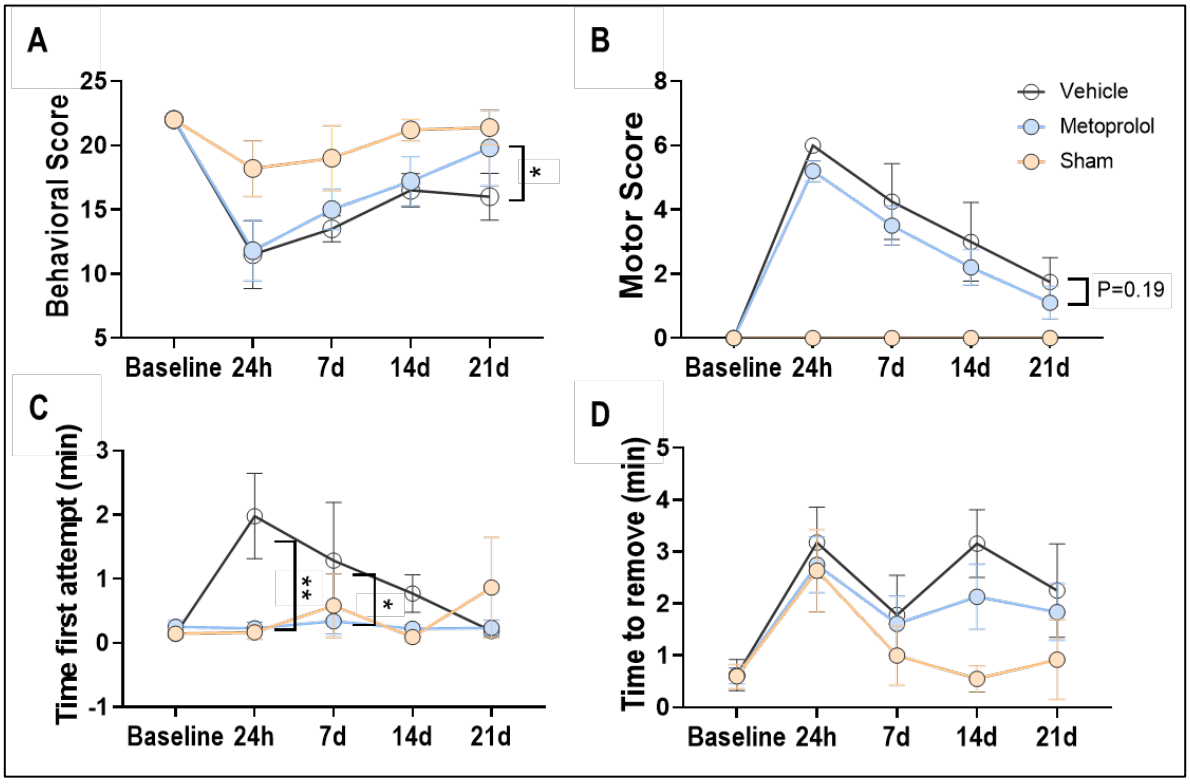

A longitudinal study was performed to evaluate long-term effects of brain injury on sensory-motor behaviors. The results obtained with the behavioral (**A**) and motor (**B**) scales showed a better neurological function in the metoprolol-treated group. Our evaluation of the sensorimotor functions using the adhesive removal test also revealed an improvement in these neurological deficits (**C, D**) in the parameter of time for the first attempt to remove the adhesive (**C**). Sham, n=5; vehicle, n=5; metoprolol, n=10; 1 rat excluded upon confirmation of the absence of artery occlusion. Data are means ± S.E.M. *p<0.05, **p<0.01; unpaired Mann-Whitney or Student *t*-test.

Supplemental Fig. 5.

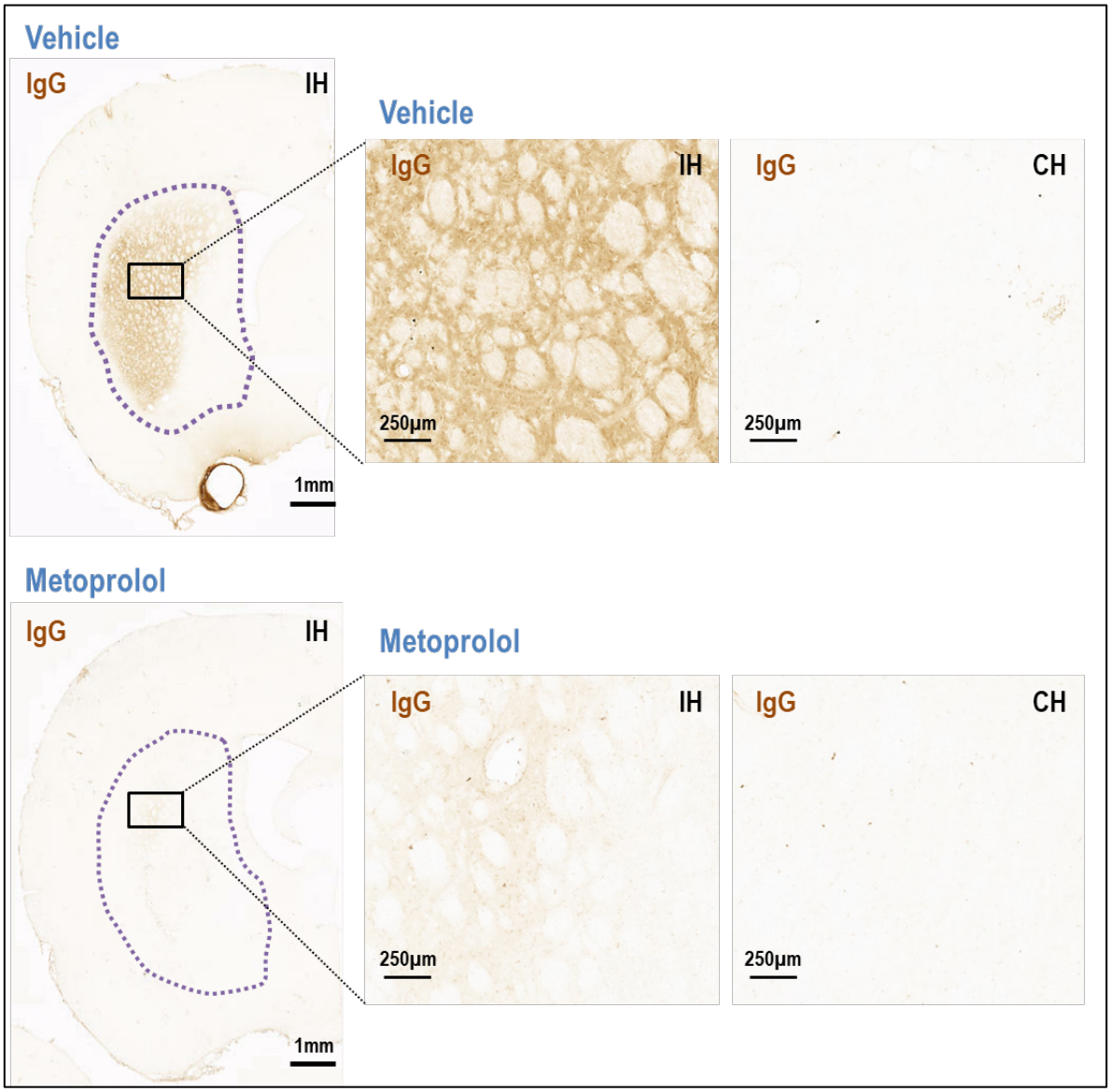

Representative IgG immunohistochemistry (IHC) on coronal sections at 7 d post-reperfusion, showing IgG extravasation in the core lesion of a vehicle-treated rat (upper panels) and its absence in a metoprolol-treated one (lower panels). IgG extravasation in the basal ganglia (outlined in purple) at 7 d post-reperfusion was attenuated in metoprolol-treated rats.

Supplemental Fig. 6.

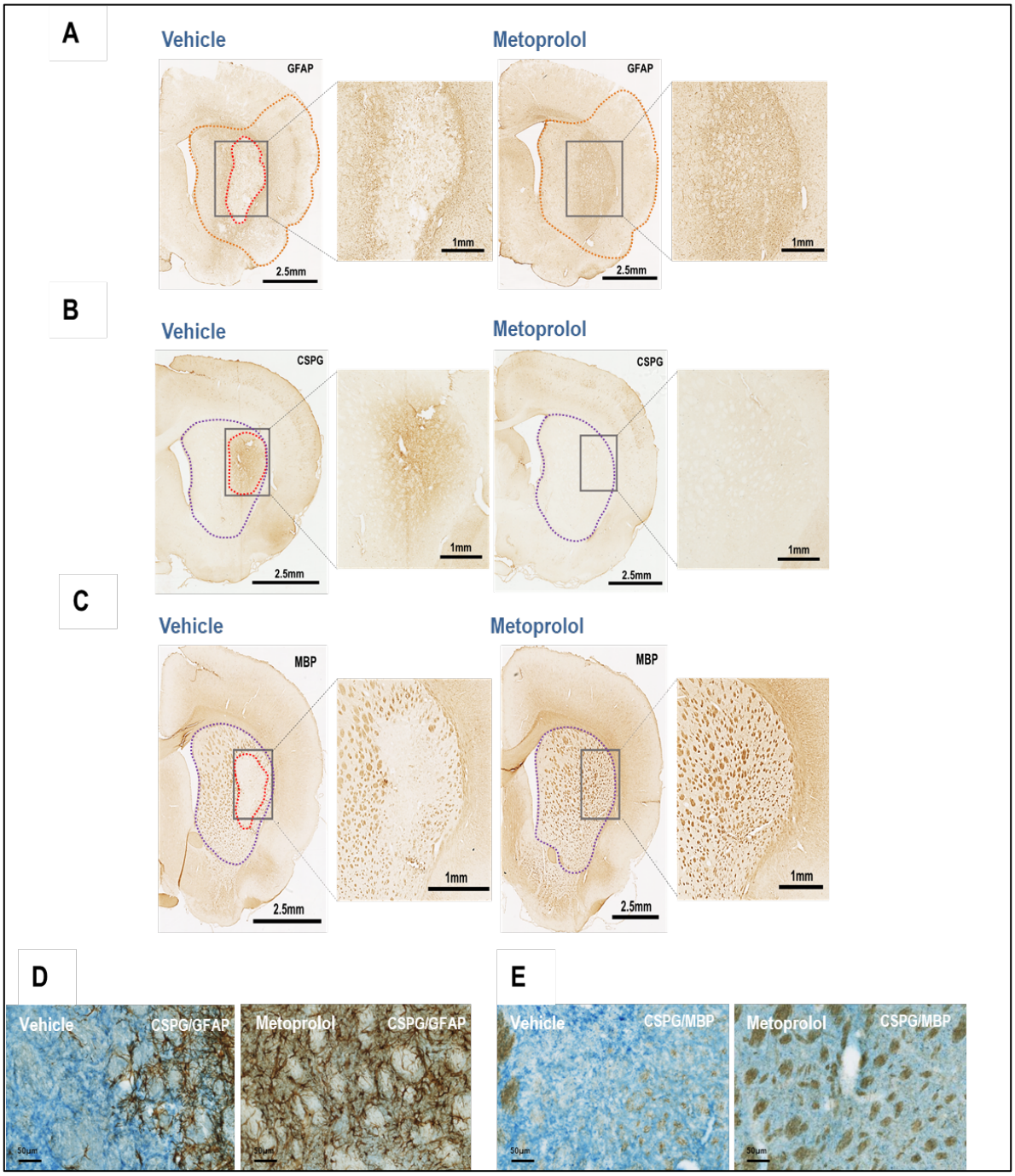

(**A**) Representative GFAP immunohistochemistry (IHC) on coronal sections at 7 d post-reperfusion, showing a glial scar (red outline) in the core lesion of a vehicle-treated rat (left) and the absence of scarring in a metoprolol-treated rat (right). Glial scar size was measured as the area lacking astrocytes in the middle cerebral artery (MCA) territory (outlined in orange) at 7 d post-reperfusion,

showing abolition of scarring in metoprolol-treated rats. (**B**) Representative IHC of chondroitin sulfate proteoglycans (CSPGs) on coronal sections at 7 d post-reperfusion, showing CSPG deposition (red outline) in the core lesion of a vehicle-treated rat (left) and its absence in a metoprolol-treated rat (right). CSPG deposition in the basal ganglia (outlined in purple) at 7 d post-reperfusion was attenuated in metoprolol-treated rats. (**C**) Representative myelin basic protein (MBP) IHC on coronal sections at 7 d post-reperfusion, showing myelin sheath degeneration in the core lesion (red outline) of a vehicle-treated rat (left) and preserved myelination in a metoprolol-treated rat (right). Quantification of basal ganglia (outlined in purple) myelin sheath degeneration at 7 d post-reperfusion shows preserved myelination in metoprolol-treated rats. High magnification views illustrate this process. (**D**) Representative double immunostaining for CSPG (blue) and GFAP (brown), showing a glial scar filled with a proteoglycan matrix in a vehicle-treated rat (left) and the absence of scarring in a metoprolol-treated rat (right). (**E**) Representative double immunostaining for CSPG (blue) and MBP (brown), showing CSPG deposition and the accumulation of myelin sheath debris in the core lesion of a vehicle-treated rat, creating an inhibitory context for axonal and neuronal regeneration. In the metoprolol-injected rat, CSPG deposition is inhibited and myelin sheaths are preserved.

Supplemental Fig. 7.

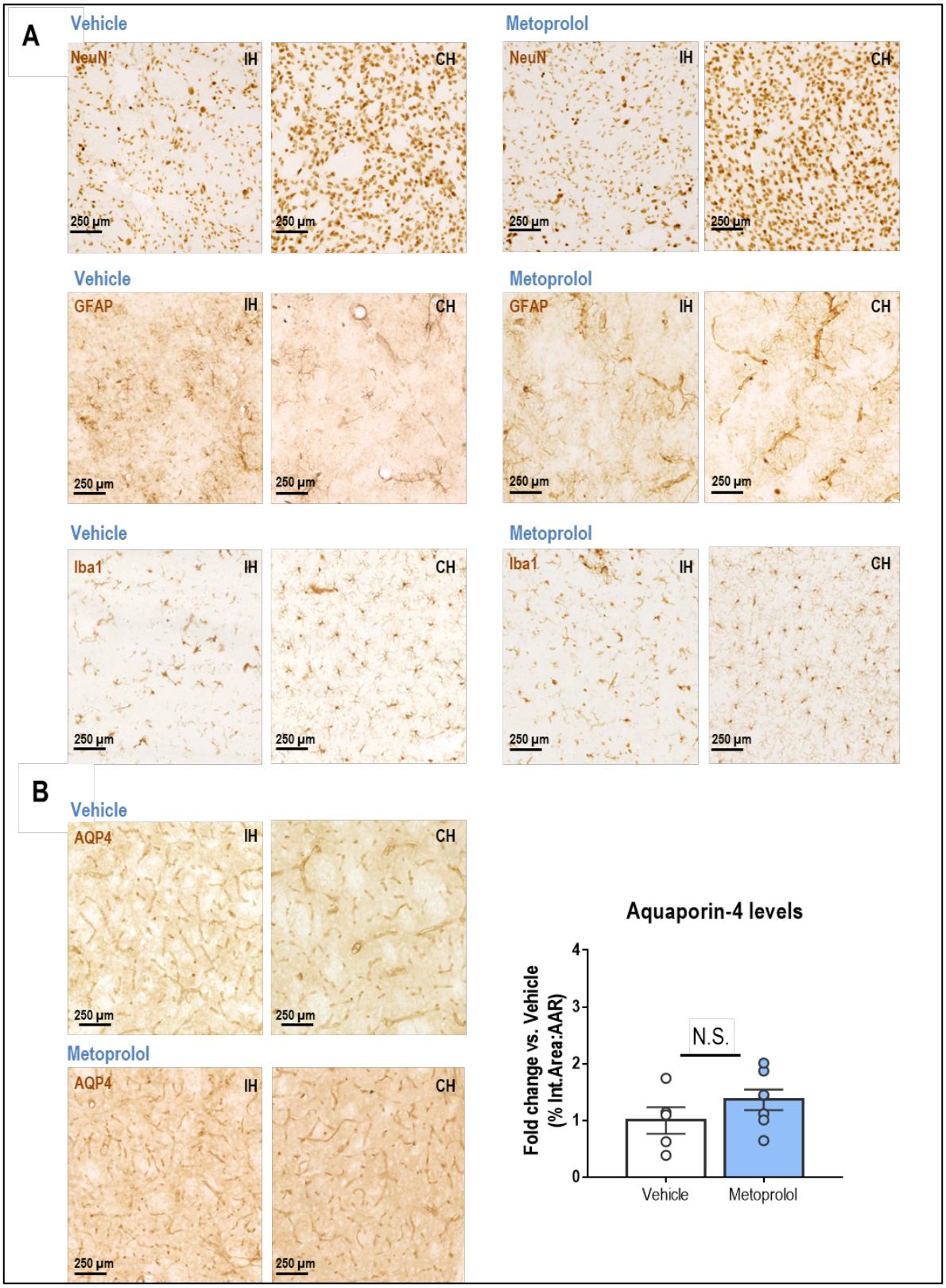

(**A**) Representative IHC of NeuN, GFAP and Iba1 on coronal sections at 24 h post-reperfusion, showing no changes in the core lesion between vehicle (left) and metoprolol (right). Neuronal nuclei lost staining and microglia started to acquire a reactive morphology; however, early after reperfusion, there is not glial scarring yet, nor microglia/macrophages pro-inflammatory response and accumulation. (**B**) Representative IHC of aquaporin 4 (AQP4) on coronal sections at 24 h post-reperfusion, which show no changes in the core lesion between vehicle (top row) and metoprolol (bottom row). Quantification of AQP4 IHC in the MCA of infarcted hemispheres shows no differences between both treatments. Vehicle, n=5; metoprolol, n=7. Graphs show mean ± S.E.M. Abbreviations as in Supplemental Fig. 3.

Supplemental Fig. 8.

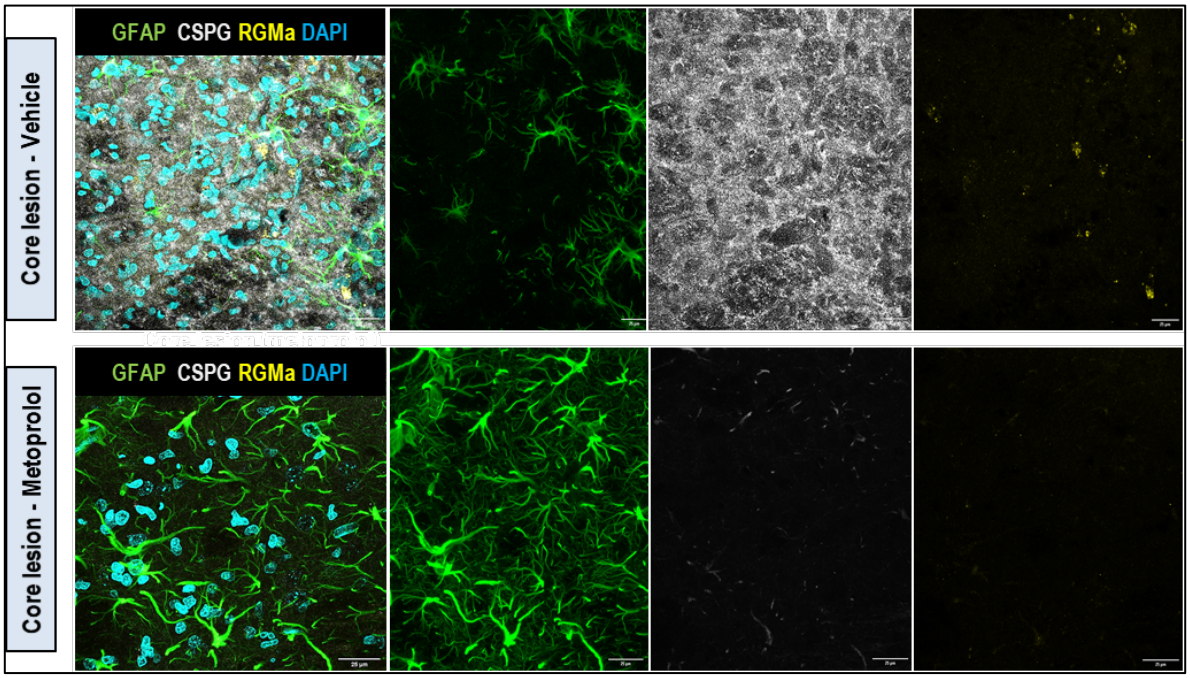

Single and merged channels of triple GFAP+CSPG+RGMa IF, showing Repulsive Guidance Molecule A expression (RGMa; **yellow**) and proteoglycan deposition (CSPG; **gray**) in the core lesion of a vehicle-treated rat (top row) and their absence in a metoprolol-treated rat (bottom row). Nuclei were revealed with DAPI (**blue**).

Supplemental Fig. 9.

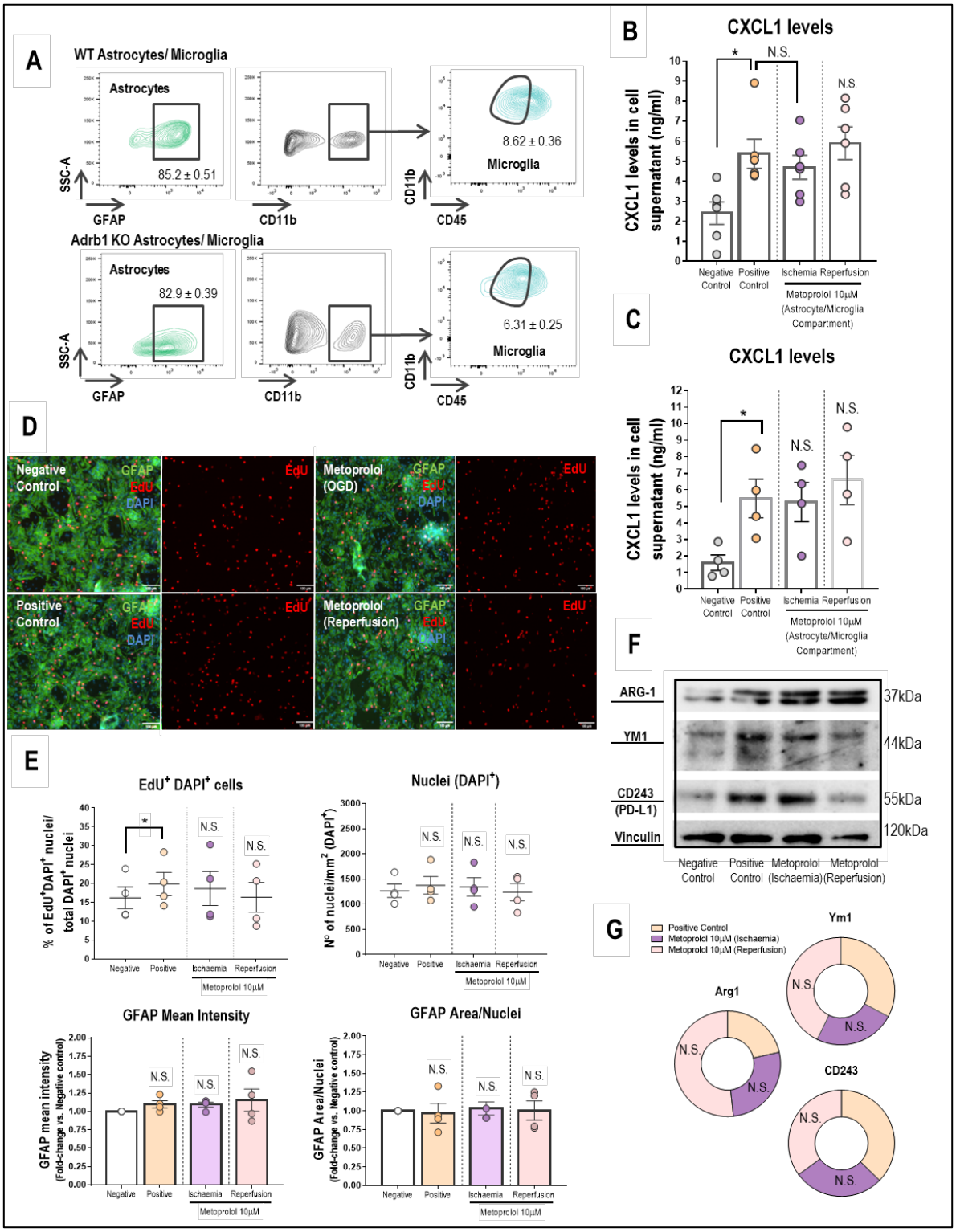

(**A**) Flow cytometry plots illustrating the purity of glia-based co-cultures. (**B, C**) CXCL1 levels in glia-based co-culture supernatants. (**D**) Fluorescence images of proliferative (EdU, **red**) astrocytes

(GFAP, **green**) subjected or not to OGD, and treated or not with vehicle or metoprolol before or after reperfusion. Nuclei were revealed with DAPI (**blue**). (**E**) Graphs show quantification of % of EdU^+ nuclei over total nuclei ($DAPI^+$), GFAP mean intensity and GFAP area/nuclei (n=4 per condition) (**F, G**) Immunoblot analyses of Arginase-1 (37 kDa), YM1 (44 kDa), CD243 (55kDa) and vinculin (120 kDa) protein expression in co-cultures subjected or not to OGD, and treated or not with vehicle or metoprolol before or after reperfusion (n=4 per condition). Graphs show mean ± S.E.M.

Supplemental Fig. 10.

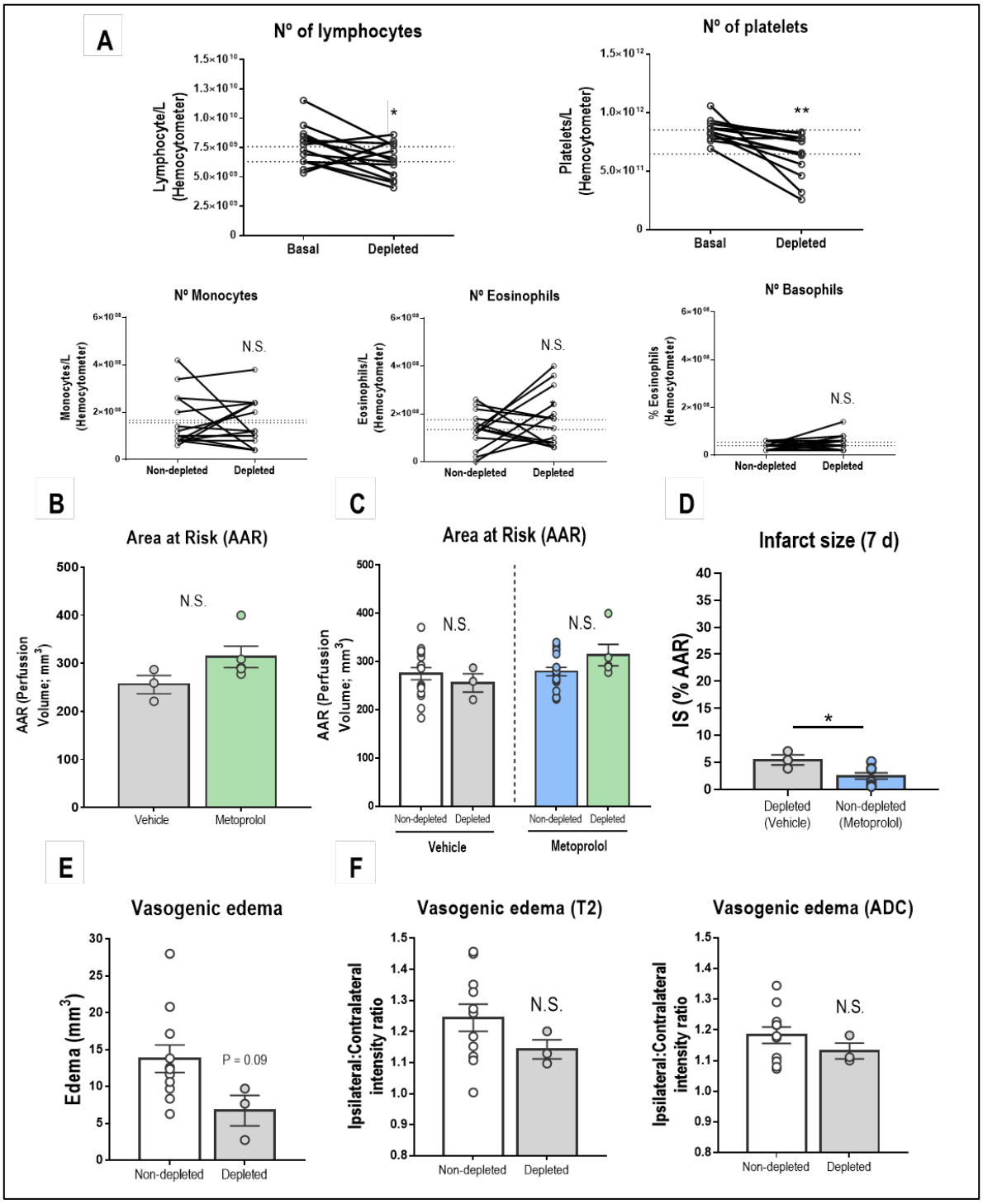

(**A**) White blood cells counts after treatment with anti-PMN serum assessed by hemocytometry. Upper and lower dotted black lines represent white blood cells counting means (baseline and after depletion). (**B, C**) Neither between distinct treatment conditions in the absence of neutrophils, nor between same treatment conditions in the presence or absence of neutrophils, differences were

observed in AAR. (**D**) The absence of neutrophils did not provide neuroprotection as metoprolol did in wild-type rats at 7 d post-reperfusion (depleted vehicle, n=3; depleted metoprolol, n=18). (**E, F**) The absence of neutrophils did not reduce vasogenic edema (non-depleted vehicle, n=16; depleted vehicle, n=3). Graphs show mean ± S.E.M. *p<0.05; **p<0.01.

VIDEO LEGENDS

Supplemental video 1. 3D confocal reconstruction of triple GFAP+AQ4+Iba1+ immunofluorescence on a coronal brain section of a rat receiving a pre-reperfusion i.v. bolus of metoprolol at 7 d post-reperfusion, illustrating preservation of aquaporin-4 expression (AQP4; **red**) in the end feet of astrocytes (GFAP; **green**), indicating preserved blood-brain barrier integrity. Microglia/macrophages (Iba1; **purple**) were found around vessels. Nuclei were revealed with DAPI (**blue**).

Supplemental videos 2. 3D confocal reconstruction of triple Neutrophil+TUNEL+Iba1+ immunofluorescence on a coronal brain section of a rat receiving a pre-reperfusion i.v. bolus of vehicle at 7 d post-reperfusion, illustrating how apoptotic (positive for TUNEL [**red**]) neutrophils (**green**) are preferably engulfed by microglia (positive for Iba1 [**gray**]). Nuclei were revealed with DAPI (**blue**).

Supplemental videos 3 (A-D). In vivo 2D IVM recordings, showing representative crawling neutrophils (positive for Ly6G [**green**] and CD62L [**yellow**]), interacting with platelets (positive for CD41 [**red**]) in inflamed cremaster muscle vessels, of WT or neutrophil conditional *Adrb1* KO mice receiving i.v. vehicle (saline) or metoprolol. Metoprolol did not provide any further effect on neutrophil behavior in the absence of β1AR.

SUPPLEMENTAL MATERIAL AND METHODS

Animals

All experimental and other scientific procedures with animals conformed to EU Directive 2010/63EU and Recommendation 2007/526/EC, enforced in Spanish law under Real Decreto 53/2013. Animal protocols were approved by the local ethics committees and the Animal Protection Area of the Comunidad Autónoma de Madrid (PROEX 056_17 and PROEX 176.3/20).

Rat procedures

Rats were maintained under pathogen-free conditions in a temperature-controlled room and a 12-hour light-dark cycle in the animal facility of Hospital General Universitario Gregorio Marañón, Madrid, Spain (ES280790000087). Chow diet and water were available ad libitum. We subjected 76 8-10-week-old wild-type male Wistar rats [RRID:RGD_737929] to middle cerebral artery occlusion during 35 min and reperfusion (MCAO/R) injury. Rats weighed around 200-250 g by the moment the stroke was induced. Animals were randomized (1:1 before initiation of surgery and blinded to the operator) to receive a pre-reperfusion 12.5 mg/kg i.v. bolus of metoprolol-tartrate (M5391, Sigma) or vehicle (saline, 0.9% NaCl) 10 min before reperfusion. A subgroup of 55 rats was monitored by MRI during MCAO (baseline) and at 24 h and 7 d post-reperfusion, followed by sacrifice and removal of the brain for immunohistochemical analysis. The remaining 21 rats were monitored under the same MRI protocol, but were sacrificed after the 24 h post-reperfusion scan for analysis of neutrophil infiltration in brain parenchyma by immunohistochemistry. The selected i.v. metoprolol dose was based on a dose-response study in rats showing a moderate hemodynamic effect (< 20%) (Garcia-Prieto et al., 2017). In the MCAO/R model, mortality reached 30% within 24 h post-reperfusion (16% and 14% for vehicle and metoprolol, respectively).

The study protocol stipulated the exclusion of rats with a quasi-hemispheric infarct (IS > 40%) at 24 h. This occurred in 9% of the rats (4% and 5% in the vehicle and metoprolol groups, respectively). MRI in these rats showed a midline shift or hemorrhage at 7 d post-reperfusion. Another animal was excluded due to a large cerebral hemorrhage at 24 h post-reperfusion. In addition, 13% of rats were excluded due to failure of the surgical model, as determined by absence of infarct on T2-weighted

(T2W) MRI images at 24 h post-reperfusion. Therefore, 46% (16 and 19 in the vehicle and metoprolol groups, respectively) of rats subjected to MCAO/R had IS <40% and were included in the evaluation of the neuroprotective effect of the early i.v. metoprolol.

To assess whether metoprolol induces neuroprotection in the absence of circulating neutrophils, an additional group of 20 rats was depleted of peripheral-blood neutrophils before MCAO/R. These animals were also monitored by MRI during MCAO, at 24 h and 7 d post-reperfusion.

Mouse procedures

Adult mice were maintained under pathogen-free conditions in a temperature-controlled room and a 12-hour light-dark cycle at the CNIC animal facility. Chow diet and water were available ad libitum. Neutrophil specific *Adrb1* knock-out (KO) mice were generated from the backcross between the Mrp8-Cre mice driver (C57BL/6 background) and the conditional Adrb1$^{flox/flox}$ (C57BL/6 background). We then obtained wild-type (WT) mice expressing β1AR (WT, Mrp8-Cre$^{/-}$ Adrb1$^{flox/flox}$) and neutrophil specific *Adrb1* KO littermates (*Adrb1* KO, Mrp8-Cre$^{/+}$ Adrb1$^{flox/flox}$).

Chemokine-induced migration transwell and intravital microscopy (IVM) were performed in 8-13-week-old male neutrophil specific *Adrb1* KO and their WT littermates. Mice were randomized to receive a single 12.5 mg/kg i.v. bolus of metoprolol-tartrate (M5391, Sigma) or vehicle (saline, 0.9% NaCl). Whole body *Adrb*1 KO mice were in a mixed background. Brains from WT or constitutive *Adrb*1 KO neonatal mice (P2-P3) were removed for astrocytes and microglia purification and growth in vitro. For neutrophil migration evaluation towards glia-based co-cultures, leukocytes were pooled from 8-13-week-old WT male C57BL/6 mice. Neonates were euthanized by decapitation and adult mice by cervical dislocation.

Cerebral ischemia-reperfusion injury

The intraluminal MCAO/R model is the gold-standard for surgical modeling of ischemic stroke. In our protocol, rats were anesthetized with 3% sevofluorane in 100% O_2 via a facemask throughout surgery and intraluminal occlusion. Immediately before surgery, animals received a single dose of 0.3 mg/kg of i.p. fentanyl. The carotid artery was then exposed, and an intraluminal 4-0 suture (Doccol,

404134PK10) was advanced via the internal carotid artery to occlude the base of the middle cerebral artery (MCA). Rats were subjected to 35 min ischemia and randomized to receive a single i.v. bolus of vehicle or metoprolol (12.5 mg/kg) 10 min before reperfusion. After the 35 min ischemia, the suture was retracted to reinstate blood flow in MCA-supplied brain territories. After incision closure, rats received 2 ml of warm saline (0.9% NaCl) subcutaneously (s.c.) as volume replacement. After the procedure, rats were placed in a warm recovery cage to prevent hypothermia, with free, easy access to food and water. To prevent pain, 0.1 mg/kg of buprenorphine was administered s.c. immediately after surgery and 24 h and 48 h post-surgery. Rats were kept under observation and monitored by MRI at different times post-reperfusion, as explained below.

Brain magnetic resonance imaging

Brain MRI scans were obtained with a 7 Tesla BioSpec 70/20 scanner (Bruker, Germany). Images were acquired using a volume coil for signal transmission and a 4-element rat-head surface coil for signal reception. Animals were maintained throughout the procedure under sevofluorane anesthesia (5% induction and 3% maintenance, in 100% O_2). Axial and coronal T2-weighted images and diffusion-weighted images (DWI) were acquired at 24 h and 7 d post-reperfusion. To assess the hypoperfusion area, a dynamic susceptibility contrast (DSC) perfusion-weighted sequence was also acquired during MCAO.

Parameters of each sequence were as follows. For T2W MRI images, a RARE sequence was acquired with TR = 6741.2 ms, TE = 30 ms, 4 averages, rare factor = 8, slice thickness = 0.4 mm, FOV = 35 x 35 mm^2, and matrix size = 256 x 256 pixels. DWI study was based on a single shot echo-planar imaging with TR = 3000ms, TE = 21 ms, 1 average, b values = 0 and 650 s/mm^2, slice thickness = 1 mm, FOV = 30 x 25 mm^2, and matrix size = 128 x 64 pixels. DSC perfusion-weighted images were dynamically acquired during an i.v. injection of 0.5mmol/kg Gd contrast agent (ProHance, Bracco Diagnostics) in 0.2 ml administered at 2.4ml/min with TR = 700 ms, TE = 7.715 ms, 1 average, 100 repetitions, slice thickness = 1 mm, FOV = 30 x 25 mm^2, and matrix size = 92 x 50 pixels.

Infarct size and edema quantification

Infarct volume at 24 h and 7 d post-reperfusion was quantified from coronal T2W MRI images. Infarct regions were selected as hyperintense areas. Area at risk (AAR) was calculated by analyzing DSC perfusion-weighted MRI images obtained during MCA occlusion, before reperfusion. Ipsilateral hypoperfused areas were detected as notably hypointense regions compared with the perfused contralateral hemisphere. Parametric apparent diffusion coefficient (ADC) maps were obtained from diffusion-weighted MRI images captured at baseline and 24 h and 7 d post-reperfusion. Cytotoxic edema (intracellular) was identified as hypointense regions, mainly observed after MCAO and at 24 h post-reperfusion. Regions of interest (ROI) were transformed into volumes by taking account of the slice thickness. Vasogenic edema (extracellular) was identified as hyperintense regions at 7 d post-reperfusion. Since vasogenic edema was mainly restricted to basal ganglia, we quantified its presence by comparing the ipsilateral (infarct) and contralateral intensities of this region in one slice per rat in ADC maps and T2WI images (-0.36/-0.96 mm Bregma interval).

Final IS was calculated as the ratio of infarct volume to the AAR. In an alternative approach, IS was calculated by considering the at-risk tissue as a perfusion-diffusion mismatch (PDM) (Butcher et al., 2008); in this approach, IS was calculated as the ratio of infarct volume to PDM. Infarct volumes estimated from T2W MRI images were also compared between groups at different time-points without normalization. MRI analyses were carried out by a blinded trained researcher.

Neurological assessment

Neurological status was assessed blinded to drug treatment, before and at different time points up to 21d after stroke (1, 7, 14 and 21d), and by the use of a motor and behavioural scales, and by the evaluation of the sensorimotor function by the use of the cylinder and the adhesive removal tests (Hunter et al., 2000; Madrigal et al., 2003; Pradillo et al., 2017; Schallert, Fleming, Leasure, Tillerson, & Bland, 2000). Within the motor scale the following neurological dysfunctions were assessed and scored: 1) no motor deficits; 2) failure to extend the contralateral forepaw fully; 3) decreased grip of contralateral forepaw while tail pulled; 4) circling to the contralateral side when tail pulled; 5) spontaneous circling or walking to the contralateral side; 6) no response to stimulation, meaning in

this scale a higher score a worse motor function. For the behavioural scale, where a lower score correlates with a poor neurological function, a combination of signs of stress and motor deficits were assessed. For the adhesive removal test, an adhesive stimulus was placed on the contralateral forepaw, leaving each animal in a new and clean cage up to 4 min. Then, the time to contact and the time to remove the adhesive stimulus were analysed. MCAO was verified by DSC images and AAR was quantified to avoid differences between groups.

Tissue processing

At 24 h and 7 d post-reperfusion, rats were anesthetized by i.p. injection of a mixture of ketamine (100mg/kg) and xylazine (5mg/kg). Rats were then transcardially perfused first with saline-heparin and second with 4% paraformaldehyde. Brains were removed and fixed in 4% paraformaldehyde for 24 h and processed for staining.

Rat brain staining and quantification

Fixed brains were cryoprotected in sucrose and frozen at -80°C. Free-floating cryostat sections (30 µm) were cut and stored in cryoprotectant buffer solution at -80°C until use. Brain infarcts extended from Bregma positions 2.04 to –2.92 mm according to the rat brain in stereotaxic coordinates atlas (Paxinos, 2007). The 3 sections analyzed per rat corresponded approximately to 3 distinct anteroposterior positions within in this brain-infarct Bregma interval. All immunohistochemical analyses therefore covered the territory affected by the MCA occlusion (Popp, Jaenisch, Witte, & Frahm, 2009; Tamura, Graham, McCulloch, & Teasdale, 1981).

Diaminobenzidine (DAB) immunohistochemical analysis was performed as previously described (Cortes-Canteli et al., 2008) using the following primary antibodies: monoclonal rabbit anti-NeuN (ab177487; Abcam) [RRID:AB_2532109], polyclonal rabbit anti-aquaporin-4 (AQP4) (A5971, Sigma-Aldrich) [RRID:AB_258270], polyclonal goat anti-ionized calcium binding adaptor molecule 1 (Iba1) (ab5076; Abcam) [RRID:AB_2224402], polyclonal rabbit anti-PMN (LSBio, LS-C348181-2), polyclonal rabbit anti-glial fibrillary acidic protein (GFAP) (Z0334, Agilent Dako, Santa Clara, CA, USA) [RRID:AB_10013382], monoclonal mouse anti-chondroitin sulfate proteoglycan (CSPG) (Cat-

315, MAB1581, Sigma-Aldrich, Merck Millipore) [RRID:AB_94270], and polyclonal rabbit anti-myelin basic protein (MBP) (GTX133108; GeneTex) [RRID:AB_2886829]. IgG extravasation analysis was performed using a goat anti-rat IgG biotinylated antibody (BA-9401-.5; Vector Laboratories) [RRID:AB_2336208]. For double immunohistochemistry (IHC), sections already stained for GFAP or MBP and developed with DAB were then incubated with the anti-CSPG antibody. The CSPG signal was detected with the ImmPRESS®-alkaline phosphatase horse anti-mouse IgG polymer detection kit (MP-5402, Vector Laboratories) [RRID:AB_2336535] and Vector Blue substrate (SK-5300, Vector Blue Alkaline Phosphatase Substrate Kit) [RRID:AB_2336837]. All IHC slides were scanned by the CNIC histopathology service using the NanoZoomer-2.0-RS digital slide scanner (C110730®, Hamamatsu, Japan) and visualized with NanoZoomer Digital Pathology software (Hamamatsu). Images were exported and quantified using ImageJ (NIH, Bethesda, MD, USA).

To determine neuronal preservation in infarcted brain hemispheres, brains removed at 7 d post-reperfusion were stained for neuronal nuclei with anti-NeuN antibody. ROIs were manually drawn to cover territories with neuronal loss. To study BBB preservation (AQP4 and IgG), CSPG deposition, myelin sheaths integrity and microglia activation, images were thresholded, and the positive area fraction in every section was averaged per rat. Glial scar formation was determined in ROIs lacking astrocyte staining and surrounded by hypertrophic astrocytes. Double-staining for CSPG plus GFAP or MBP was used to reveal filling of glial scars with proteoglycan matrix and deteriorated myelin sheaths; because proteoglycan deposition and myelin sheath degradation are largely restricted to the basal ganglia, these variables were studied in a ROI drawn around these structures. Images were then thresholded, and the mean positive area fraction was calculated from all sections and normalized to the AAR in each rat. Values were then averaged per group. Data are presented as the fold-change relative to the mean value for the vehicle-treated group. The threshold value that best highlighted the positive area was carefully selected for each marker (198 for AQ4, 215 for IgG, 220 for Iba1, 188 for CSPG and 187 for MBP), and threshold values for every marker were maintained for image quantification in all experimental groups.

For quadruple GFAP+AQP4+Iba1+CSPG immunofluorescence (IF), floating sections were blocked in PBS containing 0.25% Triton X-100 and 3% normal donkey serum and then incubated overnight at 4°C with anti-AQP4, anti-Iba1, and anti-CSPG antibodies. For triple immunofluorescence for GFAP+AQ4+Iba1, IgG+AQP4+Iba1, GFAP+MBP+NeuN, or GFAP+CSPG+RGMa, floating sections were blocked in PBS containing 0.25% Triton X-100 and 3% normal donkey serum (for anti-AQP4

and anti-Iba1) or goat serum and then incubated overnight at 4°C with anti-AQP4 plus anti-IgG, anti-Iba1, anti-MBP plus anti-NeuN, or anti-CSPG plus polyclonal rabbit anti- repulsive guidance molecule a (RGMa) (12387-1-AP, Proteintech) [RRID:AB_2179366]. After these primary antibody incubations, sections were then incubated for 1 h with the corresponding Alexa Fluor (AF)-conjugated secondary antibodies, followed by overnight incubation with mouse monoclonal anti-GFAP AF488 antibody (53989280; clone GA5; eBioscience) [RRID:AB_10597754].

Neutrophil infiltration was studied at 24 h post-reperfusion. Cells stained with anti-PMN were manually detected and quantified by IHC. PMN cells were identified according to morphology, and because blood analysis detected eosinophils and basophils at a very low proportion no distinction was made. Capillary obstruction was studied in brains removed at 24 h post-reperfusion (Bregma position -0.12/-0.60). Tissues were first rinsed in phosphate-buffered saline (PBS) and then treated with 0.2% sodium borohydride ($NaBH_4$) in PBS for 30 min and rinsed in PBS for 10 min (Liu, Connor, Peterson, Shuttleworth, & Liu, 2002; Yemisci et al., 2009) before incubation with DAPI to stain nuclei. The mean numbers of neutrophils and vascular segments with trapped erythrocytes were calculated per square millimeter and normalized to the AAR in each rat. Values were then averaged per group. Data are presented as the fold-change relative to the mean value for the vehicle-treated group.

The number of neutrophils (positive for PMN staining) expressing YM1/Chil3 was evaluated by fluorescence co-localization by using a goat polyclonal antibody anti-YM1 (AF2446, R&D Systems). For the detection of apoptotic neutrophils, a TUNEL Apoptosis Detection Kit (Green Fluorescence, KTA2010, Abbkine) was performed on brain sections (Bregma position -0.12/-0.60) following manufacturer's specifications. Next, floating sections were blocked and incubated overnight with anti-PMN and anti-Iba1, and the day after with the corresponding AF-conjugated secondary antibody. Apoptotic neutrophils were identified as positive for TUNEL staining, and the number of them being engulfed by microglia as neutrophils positive for Iba1 staining. The mean numbers of neutrophils were calculated per square millimeter and values were then averaged per group.

All slides for IF were DAPI counterstained to visualize nuclei, mounted on Superfrost Plus slides (Thermo Fisher Scientific), and covered with Fluoroshield (F6182, Sigma). Images were acquired in the CNIC Microscopy Unit with a Leica TCS SP5 or SP8 Confocal and gSTED 3D System (Leica Microsystems, Mannheim, Germany) fitted with an HC PL APO 63x/1.40 Oil CS2 objective. GFAP, AQ4, Iba1 Z-stacks were acquired with this system according to Nyquist criteria and deconvoluted

with Huygens Professional Software version 19.04.0p2 64b (Scientific Volume Imaging B.V., Hilversum, The Netherlands) using the Good's Roughness Maximum Likelihood Estimation algorithm. A 3D Surface element was created with Imaris 9.1.2 Software (Bitplane AG, Zurich, Switzerland).

Rat carotid artery catheterization and hemodynamic dose-response characterization

Animals were weighed and anesthetized (0.3 mg/kg of i.p. fentanyl, 5mg/kg midazolam and 30mg/kg alfaxalone). Systemic arterial blood pressure (BP) and heart rate (HR) were measured via a catheter (filled with heparinised saline 10U/ml) inserted through the carotid artery. This catheter was connected to a Transpac® IV (ICU Medical) pressure transducer linked to a MP36 data acquisition system and measurements were recorded using Acqknowledge data analysis software (Biopac Systems, Inc.). Crescent cumulative doses of metoprolol (3.13, 6.25, 12.5, 25, 50, 100, 150 and 200 mg/Kg) were intravenously administered via femoral artery. BP and HR were measured at baseline and 5 min after each dose administration. At the conclusion of the experiment, the catheter was removed by gently pulling it back through the stab wound, and the animal was euthanized. Animals were maintained at 36.5°C throughout the experiment.

Isolation of microglia and astrocytes from neonatal mouse brain

Mouse primary astrocyte and microglial co-cultures were prepared as previously described elsewhere (Luna-Medina et al., 2005) with some minor modifications. First, whole brains from adult C57BL/6 male WT or *Adrb*1 KO neonatal mice (P2-P3) were removed. Then, after removal of the meninges, brains were placed in sterile Hanks' balanced salt solution 1X (HBSS, 14170, Invitrogen). 6-10 brains were pooled, then washed and incubated with Trypsin 0.25% 1 h at 37ºC. To bring the reaction to a stop, we added Dulbecco's modified Eagle's medium (DMEM) supplemented with 10% fetal bovine serum (FBS) and antibiotics, and then washed twice again. Tissue was then dissociated in Ham's F-12/DMEM (1:1, 11320033, Invitrogen) containing 10% FBS and antibiotics, filtered and plated on two F-75 flasks. To promote microglia proliferation, cultures were exposed to 0.01µg/ml granulocyte-macrophage colony-stimulating factor (GM-CSF, 315-03, PreproTech). Co-cultures were then left in the incubator at 37°C and 5% CO_2 for 15 d, and media were replaced at 7 d. The purity of the astrocyte (~ 85%, $GFAP^+$) and microglial (~ 8%, $CD45^{int}CD11b^{high}$) population was determined by

flow cytometry. Astrocytes were identified by using an AF488-conjugated anti-GFAP (Clone GA5, 53989280, eBioscience) [RRID:AB_10597754], while microglia was detected by using a PE-conjugated anti-CD45 (Clone 30-F11, 560501, BD Biosciences) [RRID:AB_1645275] and AF647-conjugated anti-CD11b (Clone M1/70, 557686, BD Biosciences) [RRID:AB_396796].

Oxygen/glucose deprivation/recovery

After 15 d, flasks were trypsinized and cells were seeded in 24-well-plates. After one day, media was replaced by glucose-free DMEM (Invitrogen, 11966025) and cells were transferred into a hypoxia chamber at 1% O_2 for 1 h. At the end of oxygen/glucose deprivation (OGD), cells were replaced with Ham's F-12/DMEM and returned to the normal culture condition for 24 h. In each experiment, co-cultures exposed to OGD were compared with normoxic controls supplied with DMEM containing glucose and maintained in standard incubation conditions. Co-cultures were treated with metoprolol (10μM) throughout the OGD or during the recovery process.

Transwell assay for neutrophil migration evaluation

The capacity of neutrophils to migrate toward the chemokine C-X-C motif ligand 1 (CXCL1) was assessed using a modification of the method of Villablanca et al. (Villablanca et al., 2010) Briefly, blood from 5-6 WT mice or their neutrophil conditional *Adrb1* KO littermates was collected and filtered through a 100 μm cell strainer (352360, Falcon), and erythrocytes were lysed with hypotonic buffer (RBL buffer). Leukocytes were pooled and resuspended in RPMI containing 10% FBS and the appropriate treatment: vehicle (PBS) or metoprolol (10 μM). The lower compartments (wells) were filled with 600 μl RPMI containing 0.02 ng/μl CXCL1 (453-KC-010, R&D Systems) to induce chemoattractive movement (positive control) or with medium lacking CXCL1 to assess spontaneous migration (negative control).

To analyze the ability of neutrophils to migrate towards glia based co-cultures, the lower compartments were pre-seeded in 600μl Ham's F-12/DMEM with WT or *Adrb1* KO astrocytes and microglia, which had been previously subjected (vehicle) or not (control) to OGD conditions. Co-cultures were treated with vehicle or metoprolol (10 μM) throughout the OGD or during the recovery process. Transwell assays were not performed on co-cultures treated with metoprolol during the

recovery process to avoid the diffusion of the drug to the neutrophil chamber. A dose of 1 µg/ml of an antibody anti-CXCL1 (ab86436; abcam) was used for CXCL1 neutralization in lower chambers. Blood from 5-6 WT mice was also collected, processed as aforementioned and treated with the appropriate treatment: vehicle (PBS 1X) or metoprolol (10 µM).

Transwell inserts (6.5 mm, 5.0 µm pore size; 3421, Corning Costar Corporation) were pretreated with 50 µl RPMI for 15 min and placed in 24-well-plates before seeding cells (100 µl; ~ 0.5×10^4). After incubation at 37°C and 5% CO_2 for 90 min, cells were collected from the lower compartment, and the number of neutrophils ($Ly6G^+$ cells) was evaluated in a FACS Canto-3L flow cytometer equipped with DIVA software (BD Biosciences). Each independent experiment was conducted with leukocytes pooled from 5-6 animals, and each condition was run with 2 technical replicates. To allow comparison between experiments, in each independent experiment the migration of neutrophils was normalized per 10^4 neutrophils according to the number in the original sample of every condition.

Mouse CXCL1 ELISA

Supernatants were collected from purified WT and *Adrb1* KO astrocyte/microglia co-cultures, which had been previously subjected or not to OGD and recovery conditions, as well as metoprolol treatment before or after reperfusion. Supernatants were then used in sandwich ELISA for CXCL1 quantification (Mouse CXCL1/KC Quantikine ELISA Kit, MKC00B, R&D Systems) following manufacturer's specifications.

EdU proliferation assay

At the end of OGD, cells were replaced with Ham's F-12/DMEM containing 10µM EdU and returned to the normal culture condition for 24 h. After one day, we proceeded immediately to fix, permeabilize cells and detect EdU following manufacturer's recommendations (AF647 EdU Click Proliferation Kit, C10340, ThermoFisher). Additionally, astrocytes were stained with an AF488-conjugated anti-GFAP (Clone GA5, 53989280, eBioscience) [RRID:AB_10597754] and cell nuclei with DAPI. Fluorescent images were acquired with a Nikon Time-lapse microscope. Eight images per condition from 4 independent experiments were analyzed by a blinded observer. Images were exported and quantified

using ImageJ (NIH, Bethesda, MD, USA). Astrocyte proliferation (EdU^+ cells) was expressed as a percentage of the total number cell nuclei. $EdU^+/DAPI^+$ nuclei were quantified and related to proliferative astrocytes due to their large numbers in co-cultures (~ 85%). GFAP intensity and GFAP area/nuclei were also measured as markers of GFAP upregulation or astrocyte hypertrophy, respectively.

Immunoblotting

Cultured primary cells were collected in ice-cold RIPA buffer (R0278, Sigma) containing phosphatase and protease inhibitors. Isolated proteins were quantified by Pierce BCA Protein Assay (23225, ThermoFisher Scientific), separated by 10% SDS-PAGE, transferred to nitrocellulose membranes (Trans-Blot Turbo Transfer System, Bio-Rad), and probed with different antibodies. The following antibodies were used: anti-PD-L1 (Clone: 10F.9G2, BE0101, BioXcell) [RRID:AB_10949073], anti-YM1/Chitinase 3-like 3 (Clone: 281926, MAB2446, R&D Systems) [RRID:AB_2079007] and anti-Arginase 1 (GTX109242, GeneTex) [RRID:AB_2036264]. Vinculin was detected as a loading control (V4505, Sigma). After washes and incubation with appropriate secondary antibodies, bound antibodies were detected by enhanced chemiluminescence (ImageQuant LAS 4000 series, GE Healthcare Life Sciences), and blots were analyzed with ImageJ software (NIH, Bethesda, MD, USA).

Intravital microscopy

Intravital microscopy (IVM) of the cremaster muscle microcirculation was performed after intrascrotal injection of tumor necrosis factor-α (TNFα) (0.5μg, R&D Systems) (Sreeramkumar et al., 2014) to induce local neutrophil recruitment, followed immediately by injection of a single i.v. bolus of saline or metoprolol (12.5 mg/kg). Before cremaster muscle preparation, mice were anesthetized by i.p. injection of an anesthetic cocktail of ketamine (72 mg/kg; Anesketin Dechra, 100 mg/ml) and medetomidine hydrochloride (1 mg/kg; Domitor, 1 mg/ml). Body temperature was controlled throughout the experiment to avoid possible effects due to hypothermia. After microsurgical preparation, fluorescently labeled antibodies (0.5-1.25 μg/mouse) were administered by retro-orbital injection into the venous sinus to label surface molecules on polarized neutrophils (FITC-conjugated anti-CD62L (Clone MEL-14, 104405, BioLegend) [RRID:AB_313092] and allophycocyanin [APC]-

conjugated anti-Ly6G (Clone 1A8, BE0075-1, BioXcell) [RRID:AB_1107721]) and platelets (phycoerythrin [PE]-conjugated anti-CD41 (Clone eBioMWReg30: MWReg30, 12-0411-82 eBioscience) [RRID: AB_763486]). Fluorescence in cremester muscle venules (6-10 per mouse) was acquired for 1-2 min between 210 and 300 min after TNFα injection (Cy3/561 nm channel for PE, FITC/488 nm channel for FITC, and Cy5/640 nm channel for APC). For double staining with PE- and FITC-conjugated antibodies, acquisition was facilitated in single (FITC) and quad (PE) filters in order to avoid between-channel bleed-through of fluorescent signals.

The IVM system was built by 3i (Intelligent Imaging Innovations, Denver, CO) on an Axio Examiner Z.1 workstation (Zeiss, Oberkochen, Germany) mounted on a 3-Dimensional (3D) Motorized Stage (Sutter Instrument, Novato, CA). This set-up allows precise computer-controlled lateral movement between XY positions and a Z focusing drive for confocal acquisition. The microscope was equipped with a CoolLED pE widefield fluorescence LED light source system (CoolLED Ltd. UK) and a quad pass filter cube with a Semrock Di01-R405/488/561/635 dichroic and a FF01-446/523/600/677 emitter. We used a plan-Apochromat 40x W NA1.0 ∞/0 objective (Zeiss). Two-dimensional (2D) images were collected with a CoolSnap HQ2 camera (6.45 x 6.45-µm pixels, 1392 x 1040-pixel format; Photometrics, Tucson, AZ). Image acquisition was coordinated and offline data analysis facilitated with SlideBook software (Intelligent Imaging Innovations), run on a Dell Precision T7500 computer (Dell Inc., Round Rock, TX).

Tracking of crawling neutrophils

Kinetic properties of crawling neutrophils were studied by 2D IVM. This was crucial for testing whether the absence of β1AR directly influences the effect of metoprolol on neutrophil dynamics. Kinetic parameters of interest were velocity, accumulated and euclidean distance, and directionality. Polarized neutrophils were identified and tracked from clearly polarized morphology and uropod staining (L-selectin staining). The cell adhesion molecule L-selectin (CD62L) is expressed in a protruding microdomain at the rear of polarized leukocytes that is essential for signal integration. The CD62L-negative pole is generally known as the leading edge. Around 6-10 venules per mouse were recorded, and time-lapse videos of crawling neutrophils were analyzed with the Manual Tracking and Chemotaxis and Migration Tool plugins in ImageJ (NIH, Bethesda, MD). For each video, channel intensities were first adjusted and then converted to RGB format. Videos were rotated so that the

vessels were positioned horizontally and the blood flow oriented left-to-right. Both plugins were set up with xy calibration values, which depend on the camera and microscope parameters, to convert pixels into linear measures, as well as the time interval between video frames (3 s). Each polarized neutrophil was tracked manually 21 times (1 min) using the Manual Tracking Plugin, which generated a dataset with the respective xy track coordinates. We then used the Chemotaxis and Migration Tool to plot and to obtain neutrophil kinetic parameters for the tracks: velocity (μm/s), accumulated distance (μm), euclidean distance (μm), and directionality.

Neutrophil depletion

Neutrophils were depleted by intraperitoneal (i.p.) injection of 50μl of rabbit anti-rat polymorphonuclear cells (anti-PMN) polyclonal antibody (LSBio, LS-C348181-2) 48 h and 24 h before transient MCAO. Blood samples were drawn into EDTA tubes before (baseline) and 48 h after the first injection. Neutrophils were counted twice, by flow cytometry and hemocytometry (Pentra 80), while the rest of white blood cells were counted only by hemocytometry.

Rat peripheral neutrophils were counted by incubating cells with rabbit anti-PMN polyclonal antibody (LSBio, LS-C348181-2) and DAPI to exclude non-viable cells. Neutrophils were then incubated with Alexa Fluor 488–conjugated goat anti-rabbit secondary antibody and gated on the basis of PMN-positive staining in a FACS Canto-3L flow cytometer equipped with DIVA software (BD Biosciences). Doublet discrimination and viability (negative to DAPI) was assessed for every sample. Eosinophils and basophils were disregarded due to their minimal numbers. Data were analyzed with FlowJo software (Ashland) by blinded observers. All experiments were conducted at the CNIC Cellomics Unit.

Human neutrophil-platelet interactions evaluation

Samples and data from patients included in this study were provided by the Biobank Hospital Universitario Puerta de Hierro Majadahonda / Instituto de Investigación Sanitaria Puerta de Hierro-Segovia de Arana (IDIPHISA) (PT17/0015/0020 in the Spanish National Biobanks Network), and by Hospital Rey Juan Carlos and they were processed following standard operating procedures with the appropriate approval of the Ethics and Scientific Committees (PIC102-18_FJD-HRJC). Informed

consent was previously obtained from study participants. Metoprolol's effect on neutrophil-platelet co-aggregates was evaluated in citrated blood samples (within 24 h) from patients (> 18 years old) undergoing symptoms of ischemic stroke (< 24 h of onset, NIHSS > 3). Patients received therapy (thrombectomy, fibrinolysis or both) in the acute phase. The presence of ischemic lesion was confirmed by neuroimaging (CT or MRI, ideally) within the first 7 d of admission. Exclusion criteria were as follows: a transient ischemic attack (TIA) without ischemic lesion by neuroimaging (MRI-DWI), stroke imitators, O1-O2-O3 and S1-S2 etiologic phenotypes (ASCOD criteria), abnormal platelet (< 100.000 or > 750.000 platelets/µl) or leukocyte (< 3.000 or > 15.000 leukocytes/µl) count, history of stroke, hematologic disorder, bleeding or thrombosis, inflammatory disorder (acute outbreak within the last 2 weeks), active neoplasia, as well as chronic treatment with immunosuppressants or anti-inflammatory drugs (intake within the last 2 weeks). Blood from healthy volunteers was also drawn. Whole blood drawn was incubated *ex vivo* with metoprolol (10µM) or vehicle. Samples were then stained with a FITC-conjugated anti-CD66b (Clone: G10F5, 555724, BD Biosciences) [RRID:AB_396067], PE-conjugated anti-CD45 (Clone: HI30, 555483, BD Biosciences) [RRID:AB_395875] and PerCP-Cy5.5-conjugated anti-CD61 (Clone: VI-PL2, 564173, BD Biosciences) [RRID:AB_2738644]. Platelet ($CD61^+$ cells) and neutrophils ($CD45^+/CD66^+$ cells) were detected by flow cytometry, and neutrophils positive for CD61 staining were identified as neutrophil-platelet co-aggregates. The number of neutrophil-platelet aggregates was calculated relative to the total number of neutrophils. A sub-analysis was performed based on reperfusion confirmation in case of endovascular therapy. This sub-analysis excluded 3 patients who did not undergo recanalization. In patients who received fibrinolysis recanalization was not confirmed.

Statistics

Sample size was calculated by power analysis based on a pilot study considering the effect size (40% of reduction), standard deviation (6.5%), type 1 error (5%, P=0.05), power (80%), direction of the effect (two-tailed) and statistical tests (student t-test). Data are presented as mean ± standard error of the mean (SEM) and were analyzed with Prism software 8.0.1 (Graph pad, Inc.). Group size is the number of independent values. Statistical analysis was done using independent values and was undertaken only for studies where each group size was at least n=5, but for experiments of absence of neutrophils due to the fact that some rats were not correctly depleted by the moment of

the surgery. To reduce sources of variation, data from immunohistochemical analysis were corrected to control group values. Absence of outliers was confirmed by Grubb's test ($P < 0.05$). Normality tests (Shapiro-Wilk test) were used to determine if variables followed a normal distribution. Comparisons between two treatments (e.g. vehicle and metoprolol) were made by 2-tailed unpaired Mann-Whitney for non-normally distributed data or Student's *t*-test for variables with a normal distribution. Comparisons among more than two treatment conditions were made by 1-way ANOVA and Holm Sidak's post-hoc multiple comparisons method for normally distributed data, or by Kruskal-Wallis test and Dunn's post-hoc method for non-normally distributed. Comparisons between cell culture conditions were made by RM 1-way ANOVA and Holm Sidak's post-hoc multiple comparisons method. Comparisons between the baseline and neutrophil-depleted conditions were made by paired Student's *t*-test. Comparison between cell treatment conditions (e.g. vehicle and metoprolol) from the same patient were made by Wilcoxon Matched-Pairs Signed Ranks Test or paired Student's *t*-test for non-normally or normally distributed data, respectively. Differences were deemed statistically significant at P values below 0.05: * $p<0.05$, ** $p<0.01$, *** $p<0.001$.

REFERENCES

Butcher, K., Parsons, M., Allport, L., Lee, S. B., Barber, P. A., Tress, B., . . . Investigators, E. (2008). Rapid assessment of perfusion-diffusion mismatch. *Stroke, 39*(1), 75-81. doi: 10.1161/STROKEAHA.107.490524

Cortes-Canteli, M., Luna-Medina, R., Sanz-Sancristobal, M., Alvarez-Barrientos, A., Santos, A., & Perez-Castillo, A. (2008). CCAAT/enhancer binding protein beta deficiency provides cerebral protection following excitotoxic injury. *J Cell Sci, 121*(Pt 8), 1224-1234. doi: 10.1242/jcs.025031

Encarnacion, A., Horie, N., Keren-Gill, H., Bliss, T. M., Steinberg, G. K., & Shamloo, M. (2011). Long-term behavioral assessment of function in an experimental model for ischemic stroke. *J Neurosci Methods, 196*(2), 247-257. doi: 10.1016/j.jneumeth.2011.01.010

Garcia-Prieto, J., Villena-Gutierrez, R., Gomez, M., Bernardo, E., Pun-Garcia, A., Garcia-Lunar, I., . . . Ibanez, B. (2017). Neutrophil stunning by metoprolol reduces infarct size. *Nat Commun, 8*, 14780. doi: 10.1038/ncomms14780

Hunter, A. J., Hatcher, J., Virley, D., Nelson, P., Irving, E., Hadingham, S. J., & Parsons, A. A. (2000). Functional assessments in mice and rats after focal stroke. *Neuropharmacology, 39*(5), 806-816. doi: 10.1016/s0028-3908(99)00262-2

Liu, S., Connor, J., Peterson, S., Shuttleworth, C. W., & Liu, K. J. (2002). Direct visualization of trapped erythrocytes in rat brain after focal ischemia and reperfusion. *J Cereb Blood Flow Metab, 22*(10), 1222-1230. doi: 10.1097/01.wcb.0000037998.34930.83

Luna-Medina, R., Cortes-Canteli, M., Alonso, M., Santos, A., Martinez, A., & Perez-Castillo, A. (2005). Regulation of inflammatory response in neural cells in vitro by thiadiazolidinones derivatives through peroxisome proliferator-activated receptor gamma activation. *J Biol Chem, 280*(22), 21453-21462. doi: 10.1074/jbc.M414390200

Madrigal, J. L., Caso, J. R., de Cristobal, J., Cardenas, A., Leza, J. C., Lizasoain, I., . . . Moro, M. A. (2003). Effect of subacute and chronic immobilisation stress on the outcome of permanent focal cerebral ischaemia in rats. *Brain Res, 979*(1-2), 137-145. doi: 10.1016/s0006-8993(03)02892-0

Paxinos, G., Watson, C. . (2007). *The Rat Brain in Stereotaxic Coordinates* (6th ed.): Elsevier Inc. .

Popp, A., Jaenisch, N., Witte, O. W., & Frahm, C. (2009). Identification of ischemic regions in a rat model of stroke. *PLoS One, 4*(3), e4764. doi: 10.1371/journal.pone.0004764

Pradillo, J. M., Murray, K. N., Coutts, G. A., Moraga, A., Oroz-Gonjar, F., Boutin, H., . . . Allan, S. M. (2017). Reparative effects of interleukin-1 receptor antagonist in young and aged/co-morbid rodents after cerebral ischemia. *Brain Behav Immun, 61*, 117-126. doi: 10.1016/j.bbi.2016.11.013

Schallert, T., Fleming, S. M., Leasure, J. L., Tillerson, J. L., & Bland, S. T. (2000). CNS plasticity and assessment of forelimb sensorimotor outcome in unilateral rat models of stroke, cortical ablation, parkinsonism and spinal cord injury. *Neuropharmacology, 39*(5), 777-787. doi: 10.1016/s0028-3908(00)00005-8

Sreeramkumar, V., Adrover, J. M., Ballesteros, I., Cuartero, M. I., Rossaint, J., Bilbao, I., . . . Hidalgo, A. (2014). Neutrophils scan for activated platelets to initiate inflammation. *Science, 346*(6214), 1234-1238. doi: 10.1126/science.1256478

Tamura, A., Graham, D. I., McCulloch, J., & Teasdale, G. M. (1981). Focal cerebral ischaemia in the rat: 1. Description of technique and early neuropathological consequences following middle cerebral artery occlusion. *J Cereb Blood Flow Metab, 1*(1), 53-60. doi: 10.1038/jcbfm.1981.6

Villablanca, E. J., Raccosta, L., Zhou, D., Fontana, R., Maggioni, D., Negro, A., . . . Russo, V. (2010). Tumor-mediated liver X receptor-alpha activation inhibits CC chemokine receptor-7 expression on dendritic cells and dampens antitumor responses. *Nat Med, 16*(1), 98-105. doi: 10.1038/nm.2074

Yemisci, M., Gursoy-Ozdemir, Y., Vural, A., Can, A., Topalkara, K., & Dalkara, T. (2009). Pericyte contraction induced by oxidative-nitrative stress impairs capillary reflow despite successful opening of an occluded cerebral artery. *Nat Med, 15*(9), 1031-1037. doi: 10.1038/nm.2022